JOURNAL OF GUIDANCE, CONTROL, AND DYNAMICS
Vol. 15, No. 4, July-August 1992

# Adaptive Attitude Control and Momentum Management for Large-Angle Spacecraft Maneuvers

Alexander G. Parlos*
*Texas A&M University, College Station, Texas 77843*
and
John W. Sunkel†
*NASA Johnson Space Center, Houston, Texas 77058*

**The fully coupled equations of motion are systematically linearized around an equilibrium point of a gravity gradient stabilized spacecraft, controlled by momentum exchange devices. These equations are then used for attitude control system design of an early Space Station Freedom flight configuration, demonstrating the errors caused by the improper approximation of the spacecraft dynamics. A full state feedback controller, incorporating gain-scheduled adaptation of the attitude gains, is developed for use during spacecraft on-orbit assembly or operations characterized by significant mass properties variations. The feasibility of the gain adaptation is demonstrated via a Space Station Freedom assembly sequence case study. The attitude controller stability robustness and transient performance during gain adaptation appear satisfactory.**

## Introduction

THE desire to expand permanent human presence within and beyond our solar system will probably necessitate the design and deployment of larger, potentially more complex spacecraft than any previously flown. During their anticipated long lifetime these spacecraft will undergo significant configuration changes resulting from initial and evolutionary on-orbit assembly and from routine operations such as docking and berthing of interplanetary transportation vehicles. A representative example of such a spacecraft, incorporating multiple payloads and potentially large space platforms, as well as requiring on-orbit assembly, is the Space Station Freedom (SSF). To a certain extent these changes will affect the spacecraft attitude controller, which must maintain stable operation under these occasionally adverse conditions. Furthermore, in the case of the SSF, stable operation must be achieved only by using momentum exchange devices known as control-moment gyroscopes (CMGs), while minimizing the use of the reaction jets to conserve propellant.

A number of studies have presented the tradeoffs in selecting the various attitude control and momentum management techniques appropriate for orbiting, permanently manned space stations. A brief overview of these approaches is presented by Wie et al.[1] Various techniques based on modern control theory have been proposed, and their feasibility has been demonstrated via simulations. Most studies, however, have either been limited to spacecraft maneuvers with small-attitude deviations from the local-vertical local-horizontal (LVLH) coordinate system,[1,2] or have only partially treated attitude control and momentum management for large-angle maneuvers.[3,4] Initial observations of the potential problems regarding the attitude control of evolving and possibly asymmetric spacecraft configurations have been reported by Holmes.[5] Subsequently, independent studies have presented potential solutions to the large-angle attitude control problem of gravity gradient stabilized spacecraft.[6,7]

Expanding on previously reported work,[7] a general linearized model for a gravity gradient stabilized spacecraft is developed, which is valid around any estimated torque equilibrium attitude (TEA) value. The developed model is used for the design of a full-state feedback attitude controller for an early flight configuration of the SSF. Such configurations with significant products of inertias are anticipated early in the assembly sequence and during some of the normal spacecraft operations.[8] Computer simulations demonstrate that, without the use of a systematically developed linearized model, effective attitude control of asymmetric, gravity gradient stabilized spacecraft configurations may not be feasible. Furthermore, the use of this general linearized spacecraft model in the gain-scheduled attitude control of evolving spacecraft configurations is demonstrated. A simplified and open-loop form of adaptive control, gain scheduling appears adequate for attitude control and momentum management during significant changes in mass properties, primarily because of the inherently slow dynamics of the spacecraft configurations analyzed.

The nonlinear equations of motion for a single rigid-body, CMG-controlled, gravity gradient stabilized spacecraft are presented in the next section. The derivation of the linearized equations of motion for a similar spacecraft, valid in the vicinity of an estimated and possibly large-angle TEA value, is given in the following section. The application of the developed general linearized equations of motion to the proposed SSF attitude control and momentum management system architecture is then presented. Computer simulation results using an early SSF flight configuration attitude controller and the proposed adaptive controller are included, followed by some concluding remarks.

## Rigid-Body Nonlinear Spacecraft Dynamics

Future spacecraft are anticipated to have lifetimes on the order of 20–30 yr, while undergoing a number of evolutionary stages. For example, the SSF is expected to operate in a circular orbit at an altitude of ~200 nm, with a period of ~95 min. In reality, spacecraft such as the SSF represent flexible multibody systems subject to various external disturbances that may not be accurately known. During their assembly sequence, such spacecraft will typically undergo increasingly complex modifications as a result of the attached solar panels, thermal radiators, payloads, pressurized modules, etc. Hence, there will be an increased interaction among the various structural components and the spacecraft guidance, navigation, and con-

Received July 2, 1990; revision received Oct. 3, 1991; accepted for publication Oct. 11, 1991. 

*Assistant Professor, Department of Nuclear Engineering. Senior Member AIAA.

†Head, Space Station Control System Development & Integration. Associate Fellow AIAA.

trol system. To guarantee safe, reliable operation the spacecraft control system should be able to keep the attitude angle excursions within some yet unspecified bounds while using only the available control torque and without saturating the control actuators (in the case of the SSF the CMGs). Therefore, there is a need to systematically design attitude control systems that will have a predictable, reliable operation.

Assuming single rigid-body motion, the nonlinear equations of motion for a CMG-controlled, gravity gradient stabilized spacecraft with body-fixed control axes can be expressed as follows[1,5]:

$$I\dot{\omega}(t) = \tau_{\text{gyro}}(t) + \tau_{gg}(t) + [w(t) - u(t)] \tag{1}$$

where $\omega(t) = [\omega_1(t), \omega_2(t), \omega_3(t)]^T$ are the body-axis components of the absolute angular velocity of the spacecraft, with the subscripts 1, 2, and 3 representing the roll, pitch, and yaw axes, respectively. The matrix $I$ contains the moments of inertia $I_{ii}$, $i = 1,2,3$, as well as the products of inertia $I_{ij}$, $i = 1,2,3$ and $j = 1,2,3$, with $i \neq j$. The first two terms on the right-hand side of Eq. (1) represent the gyroscopic and gravity gradient torques. The vectors $w(t) = [w_1(t), w_2(t), w_3(t)]^T$ and $u(t) = [u_1(t), u_2(t), u_3(t)]^T$ represent the body-axis components of the external disturbance torque and the control torque resulting from the CMG momentum change, respectively.

The gyroscopic torque term is expressed in terms of the absolute angular velocities as follows:

$$\tau_{\text{gyro}}(t) = -\begin{bmatrix} 0 & -\omega_3(t) & \omega_2(t) \\ \omega_3(t) & 0 & -\omega_1(t) \\ -\omega_2(t) & \omega_1(t) & 0 \end{bmatrix} \begin{bmatrix} I_{11} & I_{12} & I_{13} \\ I_{21} & I_{22} & I_{23} \\ I_{31} & I_{32} & I_{33} \end{bmatrix} \begin{bmatrix} \omega_1(t) \\ \omega_2(t) \\ \omega_3(t) \end{bmatrix} \tag{2}$$

The gravity gradient torque term is expressed in terms of the Euler angles with respect to LVLH:

$$\tau_{gg}(t) = 3n^2 \begin{bmatrix} 0 & -c_3(t) & c_2(t) \\ c_3(t) & 0 & -c_1(t) \\ -c_2(t) & c_1(t) & 0 \end{bmatrix} \begin{bmatrix} I_{11} & I_{12} & I_{13} \\ I_{21} & I_{22} & I_{23} \\ I_{31} & I_{32} & I_{33} \end{bmatrix} \begin{bmatrix} c_1(t) \\ c_2(t) \\ c_3(t) \end{bmatrix} \tag{3}$$

where $n$ is the orbital frequency, 0.0011 rad/s for the SSF, and where the components of the nadir vector $c(t)$ are given by the following expressions:

$$\begin{aligned} c_1(t) &\equiv -\sin[\theta_2(t)] \cos[\theta_3(t)] \\ c_2(t) &\equiv \cos[\theta_1(t)] \sin[\theta_2(t)] \sin[\theta_3(t)] + \sin[\theta_1(t)] \cos[\theta_2(t)] \\ c_3(t) &\equiv -\sin[\theta_1(t)] \sin[\theta_2(t)] \sin[\theta_3(t)] + \cos[\theta_1(t)] \cos[\theta_2(t)] \end{aligned} \tag{4}$$

respectively, with $\theta_1(t)$, $\theta_2(t)$, and $\theta_3(t)$ representing the roll, pitch, and yaw angles of the spacecraft.

The attitude kinematics expresses the relation between the absolute angular velocities and the body-axis attitude rates with respect to LVLH as follows:

$$\dot{\theta}(t) = f[\theta(t)]\omega(t) + q \tag{5}$$

where

$$f[\theta(t)] = \frac{1}{\cos[\theta_3(t)]} \begin{bmatrix} \cos[\theta_3(t)] & -\cos[\theta_1(t)] \sin[\theta_3(t)] & \sin[\theta_1(t)] \sin[\theta_3(t)] \\ 0 & \cos[\theta_1(t)] & -\sin[\theta_1(t)] \\ 0 & \sin[\theta_1(t)] \cos[\theta_3(t)] & \cos[\theta_1(t)] \cos[\theta_3(t)] \end{bmatrix} \tag{6}$$

and

$$q = \begin{bmatrix} 0 \\ n \\ 0 \end{bmatrix}, \qquad \theta(t) = \begin{bmatrix} \theta_1(t) \\ \theta_2(t) \\ \theta_3(t) \end{bmatrix} \tag{7}$$

The CMG dynamics are expressed in terms of the body-axis components of the CMG momentum and the external control torque $u(t)$ commanded by the attitude control system as follows:

$$\dot{h}(t) = u(t) - \begin{bmatrix} 0 & -\omega_3(t) & \omega_2(t) \\ \omega_3(t) & 0 & -\omega_1(t) \\ -\omega_2(t) & \omega_1(t) & 0 \end{bmatrix} h(t) \tag{8}$$

The general form of the external disturbance torque used in this study is proposed in Refs. 1 and 5. That is,

$$w_i(t) = (\text{Bias})_i + A_i \sin(nt) + B_i \sin(2nt) \tag{9}$$

where $i = 1,2,3$ for the roll, pitch, and yaw, respectively.

## Derivation of the Linearized Equations of Motion

The equations of motion presented in the previous section are highly nonlinear and are therefore not suitable for systematic control system design. To allow the use of linear control system design techniques, some form of linearization must be performed. Simplified forms of the nonlinear equations of motion valid for spacecraft configurations undergoing small-attitude deviations from LVLH with negligibly small products of inertia have been successfully used for attitude control and momentum management.[1,3] However, for configurations resulting in large-angle TEA values, the applicability of this approximation will be extremely limited.[5] One approach in resolving this problem would be the linearization of the equations of motion around an estimated TEA value, an equilibrium point of the spacecraft, without decoupling the pitch from the roll/yaw equations of motion. This is justified on the basis that spacecraft exhibit large-angle TEA values because of principal inertias with comparable magnitudes in two axes, significant misalignment of the control axes with the principal axes, resulting from relatively large products of inertias, large aerodynamic torques, or a combination of these factors. Therefore, under such circumstances, assuming small-attitude deviations from LVLH and neglecting the products of inertias may result in high erroneous linearized models. Some spacecraft configurations, however, such as the SSF assembly complete (AC), will render the proposed linearization unnecessary. In these cases the derived equations, with the appropriate simplifications, become identical to the linearized equations of motion reported in the literature.[1]

### Determination of the Torque Equilibrium Attitude

To perform linearization of Eqs. (1), (5), and (8) around an equilibrium point, it is necessary to estimate the average TEA

value for a given configuration over an orbit, after equilibrium conditions have been reached. Assuming that the angles $(\theta_1^*, \theta_2^*, \theta_3^*)$ represent the estimated TEA (or the average value of the estimated TEA) value for a given configuration at steady state, these angles can be calculated using the following set of nonlinear algebraic equations:

$$\tau_{\text{gyro}}(\omega^*) + \tau_{gg}(\theta^*) + \mathbf{Bias}^* = 0 \tag{10}$$

where $\omega^*$ is the absolute angular velocity of the spacecraft evaluated at $\theta^*$, using an estimate of the aerodynamic torque vector, **Bias***, and

$$f(\theta^*)\omega^* + q = \mathbf{0} \tag{11}$$

where the function $f(\theta)$ and $q$ are defined in the previous section. The latter of these two systems of equations can be used to solve for $\omega^*$ in terms of $\theta^*$ obtaining the following relations:

$$\omega^* = \begin{bmatrix} -n\sin(\theta_3^*) \\ -n\cos(\theta_1^*)\cos(\theta_3^*) \\ n\sin(\theta_1^*)\cos(\theta_3^*) \end{bmatrix} \tag{12}$$

Substitution of these expressions into Eq. (10) reveals a system of three nonlinear algebraic equations with $(\theta_1^*, \theta_2^*, \theta_3^*)$ unknown.

The magnitude of the aerodynamic torque [the bias in Eq. (10)] and the inertia matrix $I$ must be known a priori to obtain an estimate of the TEA values by numerically solving the aforementioned system of algebraic equations. In the literature the aerodynamic torque term has been dealt with either by ignoring it during the TEA calculations[6] or by obtaining its estimate using aerodynamic models of varying complexity.[4] It has been the experience of the authors that using only approximate aerodynamic torque values for estimating the TEA does not significantly affect the spacecraft attitude transient performance. This fact has been independently reported in the literature by other researchers.[6] Nevertheless, a reasonable estimate for the aerodynamic torque has been shown to improve the transient spacecraft attitude.[4] Throughout this study, it is assumed that an estimate for the aerodynamic torque is available for use in the TEA calculations.

As previously mentioned, in addition to the aerodynamic term in Eq. (10), an estimate for the inertia matrix must also be available for obtaining TEA value estimates. For evolving spacecraft configurations, such as the ones investigated in this study, this may not be an easy task requiring on-orbit dynamic state estimation techniques. Preliminary results with a recently developed method have demonstrated that nonlinear state estimation techniques can be utilized to perform on-orbit mass properties estimation.[9] Therefore, in the rest of this study the availability of some on-orbit mass properties estimation tool will also be assumed. Furthermore, it should be noted that the TEA equations form a set of nonlinear algebraic equations, with possibly multiple equilibrium points. For a fixed pair of inertia matrix and aerodynamic torque, there are 24 spacecraft orientations that result in dynamic equilibrium.[10] In this study the TEA equations are solved using a nonlinear algebraic equation solver,[11] which requires an initial guess for the TEA values. By restricting this initial guess in the [−45 deg, +45 deg] range, a unique equilibrium point is secured. Indeed, for the spacecraft configurations of interest in this study, the TEA values are contained in this range.[12]

#### Linearization of the Attitude Kinematics

The attitude kinematics, expressed by Eq. (5), can be linearized around $(\theta^*, \omega^*)$, and the following form can be obtained:

$$\dot{\theta}(t) = \frac{1}{\cos(\theta_3^*)} \left\{ \begin{bmatrix} 0 \\ 0 \\ -n[\cos(\theta_3^*)]^2 \end{bmatrix} \delta\theta_1(t) + \begin{bmatrix} n \\ -n\sin(\theta_3^*) \\ 0 \end{bmatrix} \delta\theta_3(t) + \begin{bmatrix} \cos(\theta_3^*) \\ 0 \\ 0 \end{bmatrix} \delta\omega_1(t) + \begin{bmatrix} -\cos(\theta_1^*)\sin(\theta_3^*) \\ \cos(\theta_1^*) \\ \sin(\theta_1^*)\cos(\theta_3^*) \end{bmatrix} \delta\omega_2(t) + \begin{bmatrix} \sin(\theta_1^*)\sin(\theta_3^*) \\ -\sin(\theta_1^*) \\ \cos(\theta_1^*)\cos(\theta_3^*) \end{bmatrix} \delta\omega_3(t) \right\} \tag{13}$$

where, for $i = 1, 2, 3$,

$$\delta\theta_i(t) = \theta_i(t) - \theta_i^* \tag{14}$$

$$\delta\omega_i(t) = \omega_i(t) - \omega_i^* \tag{15}$$

represent the perturbations of the attitude angles and absolute angular velocities from the estimated TEA and from the angular velocities corresponding to the estimated TEA, respectively.

#### Linearization of the Gyroscopic Torque

The gyroscopic torque term, given by Eq. (2), can be linearized as follows:

$$\Delta\tau_{\text{gyro}}(t) = \left\{ \frac{\partial\tau_{\text{gyro}}}{\partial\omega_1}\delta\omega_1(t) + \frac{\partial\tau_{\text{gyro}}}{\partial\omega_2}\delta\omega_2(t) + \frac{\partial\tau_{\text{gyro}}}{\partial\omega_3}\delta\omega_3(t) \right\} \tag{16}$$

where each of the partial derivatives in the preceding equation, evaluated at $\theta(t) = \theta^*$, depends on the elements of the inertia matrix $I$ and the estimated TEA vector $\theta^*$. The elements of the vectors containing the partial derivatives of the gyroscopic torque with respect to the angular velocities are given in Appendix A.

#### Linearization of the Gravity Gradient Torque

The gravity gradient torque term, given by Eq. (3), can be linearized as follows:

$$\Delta\tau_{gg}(t) = \left\{ \frac{\partial\tau_{gg}}{\partial\theta_1}\delta\theta_1(t) + \frac{\partial\tau_{gg}}{\partial\theta_2}\delta\theta_2(t) + \frac{\partial\tau_{gg}}{\partial\theta_3}\delta\theta_3(t) \right\} \tag{17}$$

where each of the partial derivatives in the preceding equation, evaluated at $\theta(t) = \theta^*$, depends on the elements of $I$ and $\theta^*$. The elements of the vectors containing the partial derivatives of the gravity gradient torque with respect to the attitude angles are given in Appendix B.

#### Linearized System Equations

The preceding equations can now be assembled to form the overall linearized dynamics for the rigid-body motion of a gravity gradient stabilized spacecraft, in the vicinity of an estimated TEA vector $\theta^*$.

#### Orbital Dynamic/Kinematic Equations

The following three-dimensional vector definitions are introduced for the partial derivative terms of the external

torques to simplify the mathematical form of the final equations:

$$\tau^i_{\text{gyro}} = \frac{\partial \tau_{\text{gyro}}}{\partial \omega_i} \tag{18}$$

$$\tau^i_{gg} = \frac{\partial \tau_{gg}}{\partial \theta_i} \tag{19}$$

Each of the components of the preceding vectors corresponds to the roll, pitch, and yaw components of the external torques. Following the standard formulation used in Refs. 1, 3, 5, and 13, the following state vector is defined for the orbital dynamics and the kinematics, to be used for control system design purposes:

$$\boldsymbol{x}_1(t) = \left[\delta\omega_1(t), \dot{\theta}_2(t), \delta\omega_3(t), \delta\theta_1(t), \delta\theta_2(t), \delta\theta_3(t)\right]^T \tag{20}$$

To eliminate $\delta\omega_2(t)$ and substitute $\dot{\theta}_2(t)$ in the system equations, the kinematic relation for $\dot{\theta}_2(t)$ is substituted in the orbital dynamics. The overall linearized orbital dynamics/kinematics then take the following form:

$$\boldsymbol{E}_1 \dot{\boldsymbol{x}}_1(t) = \boldsymbol{A}_1 \boldsymbol{x}_1(t) + \boldsymbol{B}_1 \boldsymbol{u}(t) + \boldsymbol{B}_2 \boldsymbol{w}(t) \tag{21}$$

where $\boldsymbol{x}_1(t)$ is given by Eq. (20), and the matrices $\boldsymbol{E}_1$, $\boldsymbol{A}_1$, $\boldsymbol{B}_1$, and $\boldsymbol{B}_2$ are as follows:

$$\boldsymbol{E}_1 = \frac{1}{\cos(\theta_1^*)} \begin{bmatrix} I_{11}\cos(\theta_1^*) & I_{12}\cos(\theta_3^*) & I_{13}\cos(\theta_1^*)+I_{12}\sin(\theta_1^*) & 1 & 0 & 0 \\ I_{21}\cos(\theta_1^*) & I_{22}\cos(\theta_3^*) & I_{23}\cos(\theta_1^*)+I_{22}\sin(\theta_1^*) & 0 & 1 & 0 \\ I_{31}\cos(\theta_1^*) & I_{32}\cos(\theta_3^*) & I_{33}\cos(\theta_1^*)+I_{32}\sin(\theta_1^*) & 0 & 0 & 1 \\ 0 & 0 & 0 & 0 & 0 & I_{12}n\sin(\theta_3^*) \\ 0 & 0 & 0 & 0 & 0 & I_{22}n\sin(\theta_3^*) \\ 0 & 0 & 0 & 0 & 0 & I_{32}n\sin(\theta_3^*) \end{bmatrix} \tag{22}$$

$$\boldsymbol{A}_1 = \frac{1}{\cos(\theta_1^*)} \begin{bmatrix} \tau^1_{\text{gyr}}(1)\cos(\theta_1^*) & \tau^2_{\text{gyr}}(1)\cos(\theta_3^*) & \tau^3_{\text{gyr}}(1)\cos(\theta_1^*)+\tau^2_{\text{gyr}}(1)\sin(\theta_1^*) & \tau^1_{gg}(1)\cos(\theta_1^*) & \tau^2_{gg}(1)\cos(\theta_1^*) & \tau^3_{gg}(1)\cos(\theta_1^*)+\tau^2_{gg}(1)n\sin(\theta_3^*) \\ \tau^1_{\text{gyr}}(2)\cos(\theta_1^*) & \tau^2_{\text{gyr}}(2)\cos(\theta_3^*) & \tau^3_{\text{gyr}}(2)\cos(\theta_1^*)+\tau^2_{\text{gyr}}(2)\sin(\theta_1^*) & \tau^1_{gg}(2)\cos(\theta_1^*) & \tau^2_{gg}(2)\cos(\theta_1^*) & \tau^3_{gg}(2)\cos(\theta_1^*)+\tau^2_{gg}(2)n\sin(\theta_3^*) \\ \tau^1_{\text{gyr}}(3)\cos(\theta_1^*) & \tau^2_{\text{gyr}}(3)\cos(\theta_3^*) & \tau^3_{\text{gyr}}(3)\cos(\theta_1^*)+\tau^2_{\text{gyr}}(3)\sin(\theta_1^*) & \tau^1_{gg}(3)\cos(\theta_1^*) & \tau^2_{gg}(3)\cos(\theta_1^*) & \tau^3_{gg}(3)\cos(\theta_1^*)+\tau^2_{gg}(3)n\sin(\theta_3^*) \\ \cos(\theta_1^*) & -\sin(\theta_3^*)\cos(\theta_1^*) & 0 & 0 & 0 & n\cos(\theta_1^*)\frac{1-[\sin(\theta_3^*)]^2}{\cos(\theta_3^*)} \\ 0 & \cos(\theta_1^*) & 0 & 0 & 0 & 0 \\ 0 & \sin(\theta_1^*)\cos(\theta_3^*) & 1 & -n\cos(\theta_1^*)\cos(\theta_3^*) & 0 & n\sin(\theta_1^*)\sin(\theta_3^*) \end{bmatrix} \tag{23}$$

$$\boldsymbol{B}_1 = \begin{bmatrix} 1 & 0 & 0 & 0 & 0 & 0 \\ 0 & 1 & 0 & 0 & 0 & 0 \\ 0 & 0 & 1 & 0 & 0 & 0 \\ 0 & 0 & 0 & 0 & 0 & 0 \\ 0 & 0 & 0 & 0 & 0 & 0 \\ 0 & 0 & 0 & 0 & 0 & 0 \end{bmatrix}, \qquad \boldsymbol{B}_2 = -\boldsymbol{B}_1 \tag{24}$$

**Control Moment Gyroscope Dynamic Equations**

In addition to the aforementioned linearizations, the CMG dynamics can also be linearized as follows:

$$\boldsymbol{h}(t) = \boldsymbol{u}(t) - \begin{bmatrix} 0 & -\omega_3^* & \omega_2^* \\ \omega_3^* & 0 & -\omega_1^* \\ -\omega_2^* & \omega_1^* & 0 \end{bmatrix} \boldsymbol{h}(t) \tag{25}$$

where the vector $\boldsymbol{h}(t)$ represents the deviations of the CMG momentum from the nominal values at the estimated TEA and the vector $\omega^*$ is given by Eq. (12) also in terms of the estimated TEA. Because both the CMG momentum and its integral will be used in the feedback controller, the following state vector is defined for the CMGs:

$$x_2(t) = \left[h_1(t), h_2(t), h_3(t), \int h_1(t), \int h_2(t), \int h_3(t)\right]^T \tag{26}$$

Then the standard state-space form for the CMG dynamics becomes

$$xd._2(t) = \boldsymbol{A}_2 \boldsymbol{x}_2(t) + \boldsymbol{B}_2 \boldsymbol{u}(t) \tag{27}$$

where $x_2(t)$ is given by Eq. (26) and the matrix $A_2$ is given as follows:

$$A_2 = \begin{bmatrix} 0 & n\sin(\theta_1^*)\cos(\theta_3^*) & n\cos(\theta_1^*)\cos(\theta_3^*) & 0 & 0 & 0 \\ -n\sin(\theta_1^*)\cos(\theta_3^*) & 0 & -n\sin(\theta_3^*) & 0 & 0 & 0 \\ n\cos(\theta_1^*)\cos(\theta_3^*) & n\sin(\theta_3^*) & 0 & 0 & 0 & 0 \\ 1 & 0 & 0 & 0 & 0 & 0 \\ 0 & 1 & 0 & 0 & 0 & 0 \\ 0 & 0 & 1 & 0 & 0 & 0 \end{bmatrix} \tag{28}$$

**Disturbance Rejection Filter Equations**

Because the frequencies of the external disturbances are known, the following disturbance rejection filters (DRFs) can be used in the controller design for asymptotic disturbance rejection[1]:

$$\ddot{\alpha}_1(t) + n^2\alpha_1(t) = h_1(t) \tag{29}$$

$$\ddot{\alpha}_2(t) + n^2\alpha_2(t) = \delta\theta_2(t) \tag{30}$$

$$\ddot{\alpha}_3(t) + n^2\alpha_3(t) = \delta\theta_3(t) \tag{31}$$

$$\ddot{\beta}_1(t) + (2n)^2\beta_1(t) = h_1(t) \tag{32}$$

$$\ddot{\beta}_2(t) + (2n)^2\beta_2(t) = \delta\theta_2(t) \tag{33}$$

$$\ddot{\beta}_3(t) + (2n)^2\beta_3(t) = \delta\theta_3(t) \tag{34}$$

where $\alpha_i(t)$ and $\beta_i(t)$ are the filter states with arbitrary initial conditions. It is worth mentioning that the aforementioned filters are only for attitude hold. If momentum hold is desired, then a separate set of DRFs should be designed with inputs $h_1(t)$, $h_2(t)$, and $h_3(t)$. The reasons for not using $\theta_1(t)$ in the DRFs are given in Ref. 1. The preceding equations can be expressed in the following state-space form:

$$\dot{x}_3(t) = A_3x_3(t) + A_4x_1(t) + A_5x_2(t) \tag{35}$$

where $x_3(t)$ is given by

$$x_3(t) = \left[\dot{\alpha}_1(t),\alpha_1(t),\dot{\alpha}_2(t),\alpha_2(t),\dot{\alpha}_3(t),\alpha_3(t),\dot{\beta}_1(t),\beta_1(t),\dot{\beta}_2(t),\beta_2(t),\dot{\beta}_3(t),\beta_3(t)\right]^T \tag{36}$$

and where the matrices $A_3$, $A_4$, and $A_5$ are as follows:

$$A_3 = \begin{bmatrix} 0 & -n^2 & 0 & 0 & 0 & 0 & 0 & 0 & 0 & 0 & 0 & 0 \\ 1 & 0 & 0 & 0 & 0 & 0 & 0 & 0 & 0 & 0 & 0 & 0 \\ 0 & 0 & 0 & -n^2 & 0 & 0 & 0 & 0 & 0 & 0 & 0 & 0 \\ 0 & 0 & 1 & 0 & 0 & 0 & 0 & 0 & 0 & 0 & 0 & 0 \\ 0 & 0 & 0 & 0 & 0 & -n^2 & 0 & 0 & 0 & 0 & 0 & 0 \\ 0 & 0 & 0 & 0 & 1 & 0 & 0 & 0 & 0 & 0 & 0 & 0 \\ 0 & 0 & 0 & 0 & 0 & 0 & 0 & -4n^2 & 0 & 0 & 0 & 0 \\ 0 & 0 & 0 & 0 & 0 & 0 & 1 & 0 & 0 & 0 & 0 & 0 \\ 0 & 0 & 0 & 0 & 0 & 0 & 0 & 0 & 0 & -4n^2 & 0 & 0 \\ 0 & 0 & 0 & 0 & 0 & 0 & 0 & 0 & 1 & 0 & 0 & 0 \\ 0 & 0 & 0 & 0 & 0 & 0 & 0 & 0 & 0 & 0 & 0 & -4n^2 \\ 0 & 0 & 0 & 0 & 0 & 0 & 0 & 0 & 0 & 0 & 1 & 0 \end{bmatrix} \tag{37}$$

$$A_4 = \begin{bmatrix} 0 & 0 & 0 & 0 & 0 & 0 & 0 & 0 & 0 & 0 & 0 & 0 \\ 0 & 0 & 0 & 0 & 0 & 0 & 0 & 0 & 0 & 0 & 0 & 0 \\ 0 & 0 & 0 & 0 & 0 & 0 & 0 & 0 & 0 & 0 & 0 & 0 \\ 0 & 0 & 0 & 0 & 0 & 0 & 0 & 0 & 0 & 0 & 0 & 0 \\ 0 & 0 & 1 & 0 & 0 & 0 & 0 & 0 & 0 & 1 & 0 & 0 \\ 0 & 0 & 0 & 0 & 1 & 0 & 0 & 0 & 0 & 0 & 0 & 1 \end{bmatrix}^T \tag{38}$$

$$A_5 = \begin{bmatrix} 1 & 0 & 0 & 0 & 0 & 0 & 1 & 0 & 0 & 0 & 0 & 0 \\ 0 & 0 & 0 & 0 & 0 & 0 & 0 & 0 & 0 & 0 & 0 & 0 \\ 0 & 0 & 0 & 0 & 0 & 0 & 0 & 0 & 0 & 0 & 0 & 0 \\ 0 & 0 & 0 & 0 & 0 & 0 & 0 & 0 & 0 & 0 & 0 & 0 \\ 0 & 0 & 0 & 0 & 0 & 0 & 0 & 0 & 0 & 0 & 0 & 0 \\ 0 & 0 & 0 & 0 & 0 & 0 & 0 & 0 & 0 & 0 & 0 & 0 \end{bmatrix}^T \tag{39}$$

The system of Eqs. (21), (27), and (35) can now be transformed into the following state-space form:

$$\dot{x}(t) = Ax(t) + Bu(t) + Gw(t) \tag{40}$$

where the 24th-order state vector is

$$x(t) = \begin{bmatrix} x_1(t) \\ x_2(t) \\ x_3(t) \end{bmatrix} \tag{41}$$

and the system matrices $A$ (24 × 24), $B$ (24 × 3), and $G$ (24 × 3) are

$$A = \begin{bmatrix} E_1^{-1}A_1 & 0 & 0 \\ 0 & A_2 & 0 \\ A_4 & A_5 & A_3 \end{bmatrix} \tag{42}$$

$$B = \begin{bmatrix} E_1^{-1}B_1 \\ B_2 \\ 0 \end{bmatrix} \tag{43}$$

$$G = \begin{bmatrix} E_1^{-1}B_2 \\ 0 \\ 0 \end{bmatrix} \tag{44}$$

where the rest of the submatrices are previously defined and are dependent on the specific value of $\theta^*$. By setting $\theta_i^* = 0$ for $i = 1,2,3$ in Eq. (40), the equations of motion appropriate for small-attitude deviations from LVLH are obtained. Furthermore, by setting $I_{ij} = 0$, for $i \neq j$, in the same equation, the roll/yaw and pitch decoupled equations of motion are obtained. If the aforementioned two approximations are made, then the equations presented in this study are consistent with the corresponding equations of motion reported in the literature.[1,3]

## Design of an Attitude Control and Momentum Management System for Space Station Freedom

In previous sections the general equations of motion for a spacecraft [Eq. (1)], along with the kinematics and the equations for the CMGs [Eqs. (2) and (3), respectively] have been linearized around an estimated TEA value. In this section this general linear dynamic system formulation will be used to arrive at point controller designs, as well as design of an attitude control system with variable gains, functions of the spacecraft TEA value estimate, for various SSF flight configurations. It is instructive, however, to elaborate on the reasons for choosing a systematically linearized spacecraft model for the calculation of the point gains. This study addresses a potential control system architecture for a space station with evolving configurations, resulting from on-orbit assembly, human presence, docking, or berthing of a space shuttle and/or other interplanetary transportation vehicles. For a number of reasons, such as the need for continuous communications capability and proper reaction jet firing, it is desirable that the orbiting spacecraft attains and maintains LVLH attitude. However, during its planned evolutionary path or during anticipated and unanticipated scenarios, spacecraft configurations with large-angle TEA values may result. Such configurations are characterized by large roll, and/or pitch, and/or yaw angle TEA values, resulting from a combination of comparable principal inertia magnitudes in two axes, increasingly significant contributions from the products of inertias, compared to the principal inertias, and large aerodynamic torques. Under such circumstances it is still desirable to maintain system stability around an equilibrium point, the spacecraft TEA, while holding the spacecraft attitude or momentum steady.

The choice of an appropriately linearized model for attitude controller design of spacecraft configurations with large-angle TEA values appears critical. As the simulation results of this study demonstrate, a simple visual inspection of the relative magnitudes of the products of inertias with respect to the principle inertias may not be sufficient to warrant their elimination. The ultimate test involves obtaining estimates for the TEA values and checking for compliance with the assumption of small-attitude deviations from LVLH. Typically, TEA values less than ±15 deg would justify use of simplified models, based on the assumption of small-attitude deviations from LVLH. Furthermore, small-angle TEA values would indicate near-alignment of the control axes with the principal axes, justifying elimination of the products of inertias. As previously mentioned, however, large-angle TEA values could result for a number of reasons. Therefore, in addition to proper linearization, retention of the products of inertias may be necessary. Furthermore, it is highly unlikely to guarantee that the conditions for small-attitude deviations from LVLH will be satisfied for all possible configurations at the controller design stage. This indicates the possible need for on-orbit mass properties estimation as the means for obtaining TEA value estimates, which in turn could be used for scheduling the attitude controller gains. Therefore, it is desirable to have linearized mathematical models that accurately approximate the nonlinear dynamics of any spacecraft configuration for control system design purposes, should this become necessary.

The dynamic system described by Eq. (40) is used to design an attitude control system. The disturbance rejection filters proposed in Ref. 1 are used to accomplish either attitude or momentum hold, depending on the desired mode of operation. As mentioned earlier, however, only attitude hold is examined in this study. The results presented in this paper are equally applicable to the momentum hold mode, since the only change occurs in the input variables to the DRFs.

### Control System Architecture

The overall architecture of the proposed control system is shown in Fig. 1. The controller is composed of two gain-scheduled control laws: one for attitude control and momentum management and the other for rejection of the environmental disturbances. Both control laws are scheduled using the estimated average TEA value as the scheduling variable. The input signals to the controller are the attitude and attitude rates, the CMG momentum and the momentum buildup (i.e., the momentum integral), and an estimate for the average TEA value calculated using available estimates for mass properties and aerodynamic torques. The input to the DRFs consists of the attitude and momentum vectors and the TEA estimate. Because at most three independent variables can be simultaneously controlled, either the vector $[h_1(t), \delta\theta_2(t), \delta\theta_3(t)]$ or the vector $[h_1(t), h_2(t), h_3(t)]$ is used as input to the DRFs,

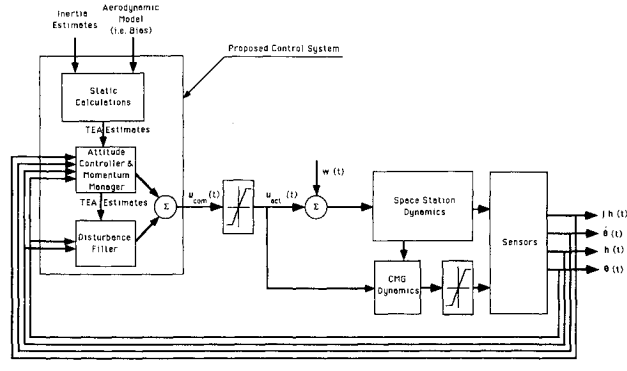


**Fig. 1 Attitude control and momentum management system architecture.**

depending on the desired operating mode of the control system.

The use of the TEA estimates in the control law is necessary because of the inadequacy of the linear control system design tools to account for the controller gain variations with changing inertia matrix elements. The static calculations involved in obtaining the TEA estimates could be performed off-line, with table lookups used during on-orbit operations. As mentioned, however, this assumes the availability of a separate module providing tabulated or dynamically estimated mass properties and aerodynamic model information. A saturation element is included as part of the simulated closed-loop system, because of the possible differences in the commanded and actual control signal that could be caused by a large control torque command. For the SSF design with six CMGs, control torque saturation occurs at 150 $lb_f$, whereas CMG saturation occurs at 20,000 ft-$lb_f$-s.

The attitude control and momentum management law used in this study is as follows:

$$u(t) = -K(\theta^*)x(t) \tag{45}$$

where the state vector $x(t)$ is given by Eq. (41) and the $3\times 24$ gain matrices $K$ are determined for various estimated TEA values, using the LQR algorithm described in the following section.

#### LQR Design with Pole Placement

Because the full state considered in Eq. (41) is available for measurement and because a minimal complexity control law is desired, the LQR is appropriate for use in obtaining the constant gains of the proposed control system. The various linear designs are performed using the dynamic system described by Eq. (40), with the elements of the system matrices evaluated at specific TEA values, corresponding to various assumed configurations of the SSF.

Assuming the state-space form of Eq. (40) with an $n$-dimensional state vector, an $m$-dimensional input vector and without the external disturbance term, the LQR problem can be stated as the minimization of the following functional:

$$J = \int_0^\infty \left[x^T(t)Qx(t) + u^T(t)Ru(t)\right] dt \tag{46}$$

where the weight matrices $Q$ and $R$ are $(n\times n)$-dimensional non-negative definite and $(m\times m)$-dimensional positive-definite symmetric matrices, respectively. The full-state feedback control law that minimizes the preceding functional is given by

$$u(t) = -Kx(t) = -R^{-1}B^TPx(t) \tag{47}$$

where $K$ is the feedback gain matrix and $P$, an $(n\times n)$-dimensional non-negative-definite symmetric matrix, is the solution of the following Riccati equation:

$$PBR^{-1}B^TP - PA - A^TP - Q = 0 \tag{48}$$

where the pair $(Q,A)$ is assumed detectable.

It is usual practice to choose the matrices $Q$ and $R$ by trial-and-error iteration, resulting in a certain gain matrix $K$ and the associated stable closed-loop poles. However, these closed-loop pole locations, although in the left-half plane, may or may not be desirable. The problem of selecting the matrices $Q$ and $R$ so that the resulting closed-loop pole locations fall in a desired sector has been widely investigated. This is the so-called LQR problem with pole placement, and it has most recently been addressed by Sunkel and Shieh.[13] Throughout this study the LQR with pole placement suggested in Ref. 13 has been used with some modifications in the solution approach of the Riccati equation. The algorithm proposed by Sunkel and Shieh[13] allows the choice of the weight matrix $R$ and the desired sector within which the closed-loop poles are to be located. The feedback gain matrix $K$ and the weight matrix $Q$, which place the closed-loop poles in the chosen sector, are then determined.

One of the numerical issues encountered in using the LQR problem for the SSF with large-angle TEA values is the solution of the associated Riccati equation. Because the order of the Riccati equation to be solved in this study is fairly high—the closed-loop system is 24th order, whereas the Hamiltonian formed is 48th order—use of the algorithms existing in the various control system design packages resulted in very inaccurate solutions. Therefore, the Riccati equation involved in the LQR with pole placement algorithm was solved using the matrix sign function,[13] with the following expression used for its evaluation:

$$\text{sign}(A) = \lim_{k\to\infty} S(k) \tag{49}$$

where $S(k)$ is determined using the following recursive expression:

$$S(k+1) = S(k)\left[5I + 10S^2(k) + S^4(k)\right]\left[I + 10S(k) + 5S^4(k)\right]^{-1} \tag{50}$$

with $S(0) = A$.

#### Gain Scheduling of the Linear Gains

Gain scheduling allows nonlinear control system implementation of linear control laws, which have been designed using any linear design method. A gain-scheduled control law is an open-loop adaptive control system.[14] Even though feedback control is used, the adaptation is open loop and the system performance may suffer. A continuous gain-scheduled control system is designed by simply fitting the various gain matrices obtained from the LQR with pole placement algorithm to a certain nonlinear function.

In view of the linearized system model of Eq. (40), the linear control law obtained by repeated application of the LQR algorithm is

$$u(t) = K_i x(t) \tag{51}$$

where $i = 1,2,\ldots$ is the number of point control systems resulting from the application of the LQR with the pole placement algorithm.

As a result of the nonlinearities involved in the gain scheduled controller, and because of the open-loop nature of the adaptation, there is no systematic procedure to determine its performance and stability characteristics, other than to exhaustively simulate the system for a variety of scenarios and for a sufficiently large number of orbits. Additionally, the stability robustness properties of the controller can only be investigated via numerical simulations. The results of these studies are presented in the following section.

## Simulation Results

The primary purpose of this section is to present some numerical simulations to substantiate the following two claims:

1) Certain spacecraft flight configurations exhibit large-angle TEA values in one or more of their three axes. For such configurations, special attention is required when selecting a linearized model for attitude control system design.

2) Because of the slowly varying nature of the SSF dynamics, a gain-scheduled control system provides "satisfactory" closed-loop performance, even for fairly large variations in the SSF inertia matrix. This results in less complex control laws compared to alternate adaptive schemes requiring on-line identification. The overall system performance, however, may suffer if the uncertainty in the inertia matrix estimates is significant.

All of the simulations presented in this section have been performed using the nonlinear simulation model of the SSF presented in prior sections of this paper. Initial conditions for all simulations were set at 1 deg for the attitude angles and 0.001 deg for the attitude rates. The rest of the states were initially assumed to be 0. Some of the simulations were also repeated with different (larger) initial attitude angles and rates, revealing similar results. No sensitivity of the reported results to initial conditions has been observed. Numerical values for the various controller gains and for the polynomial fits used in the gain scheduling can be found in Ref. 15 and are neglected in this paper for brevity.

To demonstrate the first of the two aforementioned claims, the assembly flight 3 (MB3) configuration is utilized. The MB3 corresponds to an early SSF configuration, with large pitch angle TEA value, as shown in Table 1. Nevertheless, the MB3 roll and yaw angle TEA values are negligible. It would have been possible to design an attitude control system using a spacecraft model that was linearized around an estimated pitch angle TEA, but with the roll/yaw axes linearized assuming small-attitude deviations from LVLH. However, this would have required evaluation of estimates for the TEA values of MB3, indicating that only the pitch angle TEA value is large. Alternatively, for MB3 one could argue that the $I_{12}$ and $I_{23}$ components of the inertia matrix are small compared to $I_{13}$ and can therefore be neglected. Unfortunately, this argument cannot universally be applied, because spacecraft configurations with large-angle TEA values may have relatively large products of inertias that are on the same order of magnitude.

**Table 1 Space station configuration parameters**

| Parameters | MB3 | AC |
|---|---|---|
| Inertia, slug-ft$^2$ | | |
| $I_{11}$ | $23.22\times10^6$ | $50.28\times10^6$ |
| $I_{22}$ | $1.30\times10^6$ | $10.80\times10^6$ |
| $I_{33}$ | $23.23\times10^6$ | $58.57\times10^6$ |
| $I_{12}$ | $-0.023\times10^6$ | $-0.39\times10^6$ |
| $I_{13}$ | $0.477\times10^6$ | $0.16\times10^6$ |
| $I_{23}$ | $-0.011\times10^6$ | $0.16\times10^6$ |
| TEA, deg | | |
| $\theta_1^*$ | 1.3 | 0.19 |
| $\theta_2^*$ | −44.7 | −5.0 |
| $\theta_3^*$ | 2.1 | 0.56 |

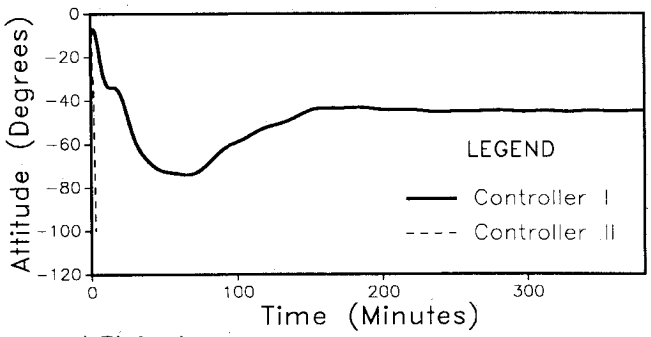


a) Pitch axis response

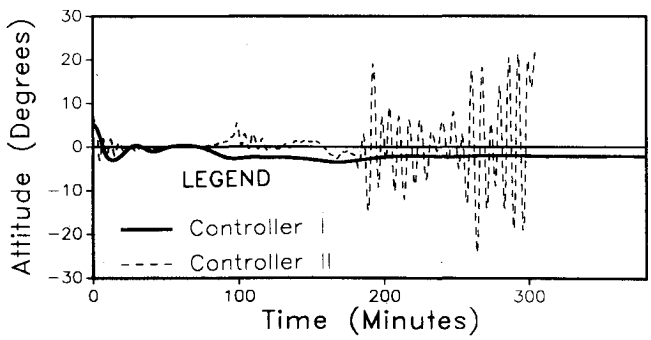


b) Yaw axis response

**Fig. 2 Pitch and yaw attitude angles for MB3 configuration.**

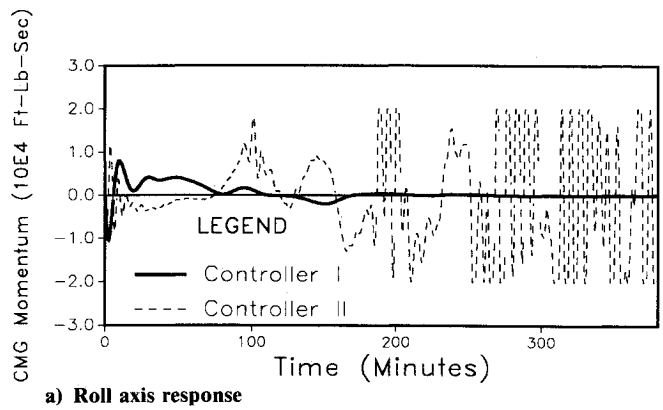


a) Roll axis response

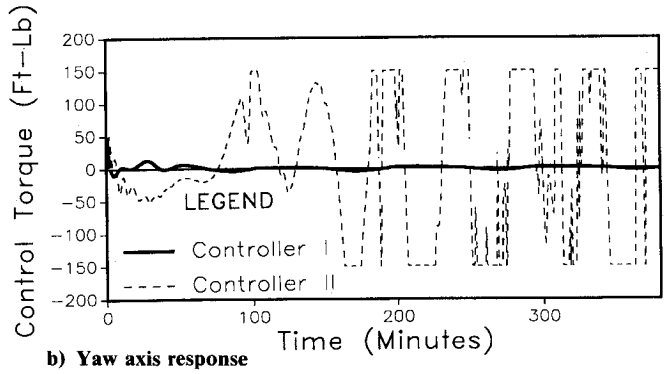


b) Yaw axis response

**Fig. 3 Roll CMG momentum and yaw control torque for MB3 configuration.**

The LQR synthesis with pole placement algorithm is used to design two controllers for the MB3 configuration. The closed-loop poles are placed in the left-half plane within the boundaries drawn by the two 45-deg lines and the $-0.5n$ vertical line, because it has been the experience of the authors that containing the closed-loop poles in this region results in relatively "good" system performance. The first controller (controller I) was designed using a linear control system based on the fully coupled roll/pitch/yaw equations of motion as described by Eq. (40), using an estimate for the TEA values. The second controller (controller II) was designed using a linearized spacecraft model that includes an estimate for the TEA value but ignores the products of inertia terms. Therefore, the second set of simulations utilized a linear control system designed using the model described by Eq. (40), with only the products of inertia terms set to zero; i.e., the assumption of small-attitude deviations from LVLH was not made. Both controllers were simulated using the same initial conditions and environmental disturbance terms. It is unnecessary to mention that both controllers resulted in stable closed-loop systems, when simulated with the linear spacecraft models used in the controller synthesis steps. Furthermore, a third controller was designed using a model similar to the one used to design controller II, with the additional assumption of small-attitude deviations from LVLH. The results for this controller were similar to those obtained using controller II; thus, they are not presented here.

Some of the simulation results for these two controllers are shown in Figs. 2 and 3. Figure 2 depicts the pitch and yaw angles, whereas Fig. 3 depicts the roll CMG momentum and the yaw control torque for the MB3 configuration, when the two aforementioned controllers are utilized. These studies clearly demonstrate the error introduced when the products of inertias of certain flight configurations are arbitrarily discarded. The transient response of the closed-loop system becomes unstable within less than one-tenth of an orbit unless the products of inertias are used in the control synthesis. The

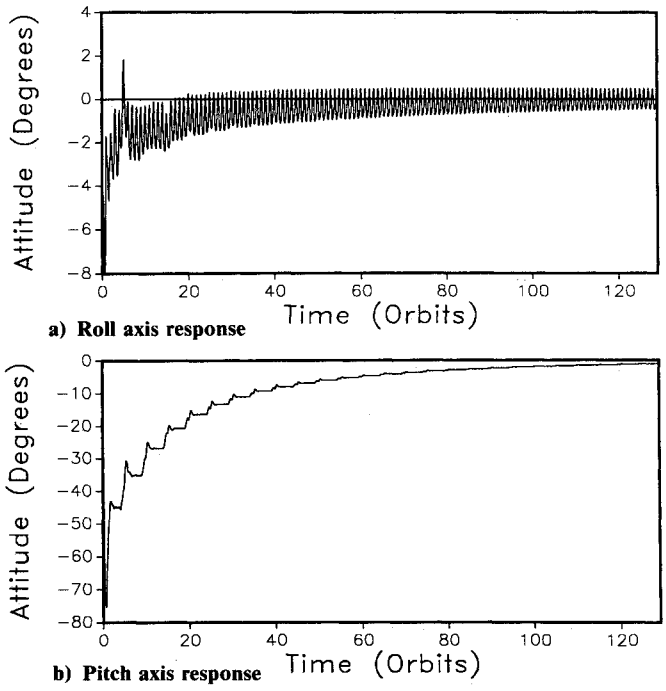


**Fig. 4 Roll and pitch attitude angles during the compressed schedule assembly sequence.**

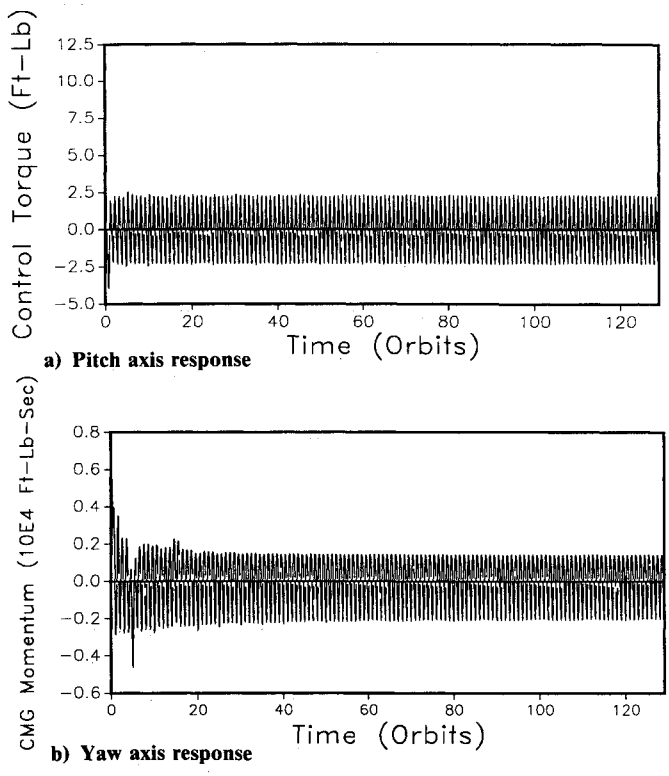


**Fig. 5 Pitch control torque and yaw CMG momentum during the compressed schedule assembly sequence.**

instability caused by controller II can be attributed to the large pitch angle TEA, resulting from the relatively large products of inertia (especially $I_{13}$ for the MB3), and to a lesser degree from the difference $(I_{11} - I_{33})$ and the aerodynamic torque. The control system design for such flight configurations requires the use of linearized models that are valid around estimated TEA values, because linear models based on small-attitude deviations from LVLH do not adequately describe the nonlinear spacecraft behavior. Furthermore, the products of inertias must be retained to account for the full three-axis coupling. It is worth noting that further tuning of the closed-loop pole locations for controller I could perhaps improve its transient response, resulting in smaller-attitude excursions. However, such design improvements are beyond the scope of this study. Additionally, numerical robustness studies have revealed that the closed-loop system with controller I remains stable for up to $\pm 30\%$ variations in the SSF inertia matrix, as previously reported in the literature.[1]

Demonstration of the second claim proved to be more time consuming and computationally more intensive. To arrive at a gain-scheduled controller, seven linear designs were performed using the LQR with pole placement, for various SSF configurations with TEA values ranging up to $-45$ deg, as shown in Table 1. Contrary to the MB3 configuration, the AC represents a highly symmetric spacecraft with small-angle TEA values. The seven SSF configurations used in the controller gain scheduling have inertia matrices with elements that are significantly different. Specifically, as observed from Table 1, which depicts the first and seventh configurations used, the inertia matrix element that exhibits the most change is $I_{12}$ (approximately a 1600% difference between the MB3 and AC configurations). First- and second-order polynomials were used in this study to schedule the elements of the gain matrices resulting from the point controller designs. Furthermore, the magnitudes of the disturbance vector components were allowed to vary, reflecting the changes in the SSF configurations, whereas the frequencies of the cyclic components were assumed to be constant. Because of the presence of the DRFs in the controller architecture, the effects of changing the cyclic component magnitudes of the disturbance vector on the control system performance are insignificant. However, the same cannot be said about the magnitude of the bias term, because it impacts the TEA values.

The gain-scheduled closed-loop dynamics were simulated for 130 orbits while the inertia matrix, corresponding to 26 different SSF configurations,[12] was allowed to change stepwise every four orbits simulating transition from one flight configuration to another. This scenario indeed imposes very fast, frequent changes in the inertia matrix. However, because of computational considerations the on-orbit assembly schedule has been compressed. Slower, less frequent variations in the inertia matrix should result in improved controller transient response. Some of the results from this set of simulations are presented in Figs. 4 and 5. Figure 4 depicts the SSF roll and pitch angle transient responses during the aforementioned compressed schedule assembly sequence using the gain-scheduled controller, whereas Fig. 5 depicts the pitch control torque and yaw CMG momentum for the same scenario. These transient responses indicate that a gain-scheduled controller, whether it is in table lookup form or a continuous polynomial, is sufficient for handling large changes in the SSF inertia matrix, including configurations that are characterized by large-angle TEA values. This is primarily attributed to the slowly varying dynamics of the SSF, with characteristic time constants on the order of tens of minutes.

## Conclusions

A systematic derivation of the linearized dynamics of a gravity gradient stabilized spacecraft around an estimated TEA is presented. The need for using a three-axis coupled spacecraft model in the development of attitude control laws for large-angle maneuvers is demonstrated via the case study of a SSF early flight configuration. Failure to use a properly approximated model that adequately describes the nonlinear spacecraft behavior during large-angle maneuvers results in attitude instabilities, detectable only by nonlinear simulations. Furthermore, a gain-scheduled adaptive controller based on full-state feedback is proposed for attitude control of spacecraft undergoing mass properties variations. The feasibility of this controller is demonstrated via the case study of a compressed assembly sequence schedule for the Space Station Freedom.

## Appendix A: Derivatives of the Gyroscopic Torque

The partial derivatives of the gyroscopic torque term, with respect to the absolute angular velocity of the spacecraft, are given by the following expressions:

$$\frac{\partial \tau_{\text{gyro}}}{\partial \omega_1} = -n\begin{bmatrix} -I_{12}\sin(\theta_1^*)\cos(\theta_3^*) - I_{13}\cos(\theta_1^*)\cos(\theta_3^*) \\ 2I_{13}\sin(\theta_3^*) + I_{23}\cos(\theta_1^*)\cos(\theta_3^*) + (I_{11}-I_{33})\sin(\theta_1^*)\cos(\theta_3^*) \\ I_{23}\sin(\theta_1^*)\cos(\theta_3^*) - 2I_{12}\sin(\theta_3^*) + (I_{11}-I_{22})\cos(\theta_1^*)\cos(\theta_3^*) \end{bmatrix} \tag{A1}$$

$$\frac{\partial \tau_{\text{gyro}}}{\partial \omega_2} = -n\begin{bmatrix} -2I_{23}\cos(\theta_1^*)\cos(\theta_3^*) - I_{13}\sin(\theta_3^*) + (I_{33}-I_{22})\sin(\theta_1^*)\cos(\theta_3^*) \\ I_{12}\sin(\theta_1^*)\cos(\theta_3^*) + I_{23}\sin(\theta_3^*) \\ 2I_{12}\cos(\theta_1^*)\cos(\theta_3^*) - I_{13}\sin(\theta_1^*)\cos(\theta_3^*) + (I_{11}-I_{22})\sin(\theta_3^*) \end{bmatrix} \tag{A2}$$

$$\frac{\partial \tau_{\text{gyro}}}{\partial \omega_3} = -n\begin{bmatrix} I_{12}\sin(\theta_3^*) - 2I_{23}\sin(\theta_1^*)\cos(\theta_3^*) + (I_{22}-I_{33})\cos(\theta_1^*)\cos(\theta_3^*) \\ -I_{12}\cos(\theta_1^*)\cos(\theta_3^*) + 2I_{13}\sin(\theta_1^*)\cos(\theta_3^*) + (I_{33}-I_{11})\sin(\theta_3^*) \\ I_{13}\cos(\theta_1^*)\cos(\theta_3^*) - I_{23}\sin(\theta_3^*) \end{bmatrix} \tag{A3}$$

## Appendix B: Derivatives of the Gravity Gradient Torque

The partial derivatives of the gravity gradient torque term, with respect to the spacecraft attitude angles, are given by the following expressions:

$$\frac{\partial \tau_{gg}}{\partial \theta_1} = -3n^2\begin{bmatrix} (-I_{12}A_1 + I_{13}B_1)C_1 + (I_{22}-I_{33})(A_1^2 - B_1^2) - 4I_{23}A_1B_1 \\ (I_{11}-I_{33})A_1C_1 + I_{12}(B_1^2 - A_1^2) + 2I_{13}A_1B_1 \\ \{(I_{22}-I_{11})B_1 + I_{23}A_1\}C_1 + I_{13}(A_1^2 - B_1^2) + 2I_{12}A_1B_1 \end{bmatrix} \tag{B1}$$

$$\frac{\partial \tau_{gg}}{\partial \theta_2} = -3n^2\begin{bmatrix} -I_{12}(A_2C_1 + C_2B_1) + I_{13}(B_2C_1 - C_2A_1) + I_{22}(A_1A_2 - B_1B_2) - I_{33}(B_1B_2 + A_1A_2) - 2I_{23}(A_2B_1 + A_1B_2) \\ I_{11}(B_1C_2 - C_1A_2) - I_{33}(A_2C_1 - B_1C_2) + I_{12}(B_1B_2 - A_1A_2) + 2I_{13}(C_1C_2 + A_2B_1) + I_{23}(A_1C_2 + C_1B_2) \\ I_{11}(A_1C_2 + B_2C_1) - I_{22}(A_1C_2 + C_1B_2) + I_{23}(B_1C_2 - C_1A_2) + I_{13}(A_1A_2 - B_1B_2) + 2I_{12}(A_1B_2 - C_1C_2) \end{bmatrix} \tag{B2}$$

$$\frac{\partial \tau_{gg}}{\partial \theta_3} = -3n^2\begin{bmatrix} (I_{22}-I_{33})(A_1A_3 - B_1B_3) - I_{12}(A_3C_1 - B_1C_3) - 2I_{23}(A_3B_1 + A_1B_3) - I_{13}(B_3C_1 + A_1C_3) \\ (I_{33}-I_{11})(A_3C_1 - B_1C_3) - I_{12}(A_1A_3 - B_1B_3) + 2I_{13}(A_3B_1 + C_1C_3) + I_{23}(A_1C_3 + B_3C_1) \\ (I_{11}-I_{22})(A_1C_3 + B_3C_1) + I_{23}(B_1C_3 - A_3C_1) + I_{13}(B_1B_3 + A_1A_3) + 2I_{12}(A_1B_3 - C_1C_3) \end{bmatrix} \tag{B3}$$

where

$$A_1 = \cos(\theta_1^*)\sin(\theta_2^*)\sin(\theta_3^*) + \sin(\theta_1^*)\cos(\theta_2^*) \tag{B4}$$

$$B_1 = \sin(\theta_1^*)\sin(\theta_2^*)\sin(\theta_3^*) - \cos(\theta_1^*)\cos(\theta_2^*) \tag{B5}$$

$$C_1 = \sin(\theta_2^*)\cos(\theta_3^*) \tag{B6}$$

$$A_2 = \sin(\theta_1^*)\cos(\theta_2^*)\sin(\theta_3^*) + \cos(\theta_1^*)\sin(\theta_2^*) \tag{B7}$$

$$B_2 = -\cos(\theta_1^*)\cos(\theta_2^*)\sin(\theta_3^*) + \sin(\theta_1^*)\sin(\theta_2^*) \tag{B8}$$

$$C_2 = \cos(\theta_2^*)\cos(\theta_3^*) \tag{B9}$$

$$A_3 = \sin(\theta_1^*)\sin(\theta_2^*)\cos(\theta_3^*) \tag{B10}$$

$$B_3 = -\cos(\theta_1^*)\sin(\theta_2^*)\cos(\theta_3^*) \tag{B11}$$

$$C_3 = -\sin(\theta_2^*)\sin(\theta_3^*) \tag{B12}$$

## Acknowledgments

The authors greatly appreciate the financial support provided by NASA Johnson Space Center Grant NAG 9-275 and NAG 9-347 to Texas A&M University.

## References

[1]Wie, B., Byun, K. W., Warren, V. W., Geller, D., Long, D., and Sunkel, J., "New Approach to Attitude/Momentum Control for the Space Station," *Journal of Guidance, Control, and Dynamics,* Vol. 12, No. 5, 1989, pp. 714–722.

[2]Harduvel, J. T., "Continuous Momentum Management of Earth-Oriented Spacecraft," *Proceedings of the AIAA Guidance, Navigation, and Control Conference,* AIAA, Washington, DC, 1990; also, AIAA Paper 90-3315, Aug. 1990, pp. 1–11.

[3]Warren, W., Wie, B., and Geller, D., "Periodic-Disturbance Accommodating Control of the Space Station for Asymptotic Momentum Management," *Journal of Guidance, Control, and Dynamics,* Vol. 13, No. 6, 1990, pp. 984–992.

[4]Kumar, R. R., Heck, M. L., and Robertson, B. P., "Predicted Torque Equilibrium Attitude Utilization for Space Station Attitude Control," *Proceedings of the AIAA Guidance, Navigation, and Control Conference,* AIAA, Washington, DC, 1990; also, AIAA Paper 90-3318, Aug. 1990.

[5]Holmes, E., "The Limitations of Linearization Techniques on Nonlinear Space Station Equations of Motion," Grumman Space Station Engineering Integration Contractor, Rept. PSH-341-RP89-002, Reston, VA, Aug. 1989.

[6]Mapar, J., "An Innovative Approach to the Momentum Management Control for Space Station Freedom," *Proceedings of the AIAA Guidance, Navigation, and Control Conference,* AIAA, Washington, DC, 1990; also, AIAA Paper 90-3317, Aug. 1990.

[7]Parlos, A. G., and Sunkel, J. W., "Attitude Control/Momentum Management of the Space Station Freedom for Large Angle Torque-Equilibrium-Attitude Configurations," *Proceedings of the AIAA Guidance, Navigation, and Control Conference,* AIAA, Washington, DC, 1990; also, AIAA Paper 90-3352, Aug. 1990.

[8]Impact of Mobile Remote Manipulator System Operations on Attitude Control/Momentum Management System Performance and Design for Phase I Complete Space Station," Dynacs Engineering Co., Clearwater, FL, Rept. prepared for NASA Johnson Space Center, Nov. 1988.

[9]Parlos, A. G., Atiya, A. F., and Sunkel, J. W., "Parameter Estimation in Space Systems Using Recurrent Neural Networks," *Proceedings of the AIAA Guidance, Navigation, and Control Confer-*

*ence,* AIAA, Washington, DC, 1991; also, AIAA Paper 91-2716, Aug. 1991.

[10]Hughes, P. C., *Spacecraft Attitude Dynamics,* Wiley, New York, 1986.

[11]"FORTRAN Subroutines for Mathematical Applications, User's Manual, MATH/LIBRARY, Version 1.1," International Mathematical and Statistical Libraries, Inc., Houston, TX, Aug. 1989.

[12]"Space Station Stage Summary Databook," Space Station Freedom Program Office, Reston, VA, Rept. prepared by Space Station Engineering Integration Contractor (SSEIC), Dec. 1989.

[13]Sunkel, J. W., and Shieh, L. S., "An Optimal Momentum Management Controller for the Space Station," *Proceedings of the AIAA Guidance, Navigation, and Control Conference,* AIAA, Washington, DC, 1989; also AIAA Paper 89-3473, Aug. 1989.

[14]Astrom, K. J., and Wittenmark, B., *Adaptive Control,* Addison-Wesley, Reading, MA, 1989.

[15]Parlos, A. G., "A Gain-Scheduled Control System Design for Attitude/Momentum Control and Stabilization of the Space Station Freedom," Decision and Information Systems Lab., Texas A&M Univ., TR 90-AS-01, College Station, TX, Jan. 1990.